CHROMOSPHERIC OSCILLATIONS

B.W. LITES
High Altitude Observatory, NCAR, Boulder, USA

R.J. RUTTEN
Sterrekundig Instituut, Utrecht, The Netherlands

and

J.H. THOMAS
University of Rochester, Rochester, USA

Abstract. We show results from NSO/Sacramento Peak data to discuss three issues:
(i)—the spatial occurrence of chromospheric 3–min oscillations;
(ii)—the validity of Ca II H & K line-center Doppler Shift measurements;
(iii)—the significance of oscillation power and phase at frequencies above 10 mHz.

Key words: sun: chromosphere, sun: oscillations, lines: formation, atmosphere: seeing

1. Introduction

While helioseismology digs down below the solar surface, interest in the physics of solar surface oscillations rises from the photosphere to the chromosphere. Major questions are:

- do upward wave propagation, shock formation and shock interference occur in the actual sun as they do in radiation hydrodynamics simulations (Rammacher and Ulmschneider, 1992; Carlsson and Stein, 1992; Fleck and Schmitz, 1993; Kalkofen *et al.*, 1994)?
- are oscillations the prime structuring agent of the quiet Sun internetwork chromosphere, or do internetwork magnetic fields or thermal inhomogeneities also play a role? In particular, do Ca II "grains" mark sites of enhanced field strength (Sivaraman and Livingston, 1982) or simply constructive interference of oscillations (Rutten and Uitenbroek, 1991; Kulaczewski, 1992), and how and where do Ayres' cool CO clouds figure in internetwork dynamics (*e.g.,* Ayres, 1991)?
- what sources drive chromospheric oscillations? Are they localized, identifiable pistons in the photosphere, such as 5–min amplitude peaks (Fleck and Schmitz, 1993), or are they to be sought in subsurface turbulent convection (Kumar, 1994)?
- is the "basal flux" which delimits stellar Ca II H & K emission due to acoustic internetwork heating (*e.g.,* Schrijver, 1992)?
- what are the dynamics of magnetic elements in the chromosphere? In particular, what motions constitute the low-frequency power of network elements (*e.g.,* Lites

[0] Appeared in: "Solar Surface Magnetism", Eds. R.J. Rutten and C.J. Schrijver, Procs. Soesterberg Workshop, NATO ASI Series C 433, Kluwer, Dordrecht, pp. 159-167. Preprint: `http://www.astro.uu.nl/~rutten/`

et al., 1993) and what causes the non-linear nature of umbral flashes (cf. Lites, 1992)?

We won't give a definitive answer to any of these questions in this contribution, but we discuss three observation-oriented topics that bear on each, from data assembled to study chromospheric dynamics with good resolution in height. A more detailed analysis will be published elsewhere. Here we note apparent large-scale spatial variations in the occurrence of quiet Sun fluctuations with 2–4 min periodicity, we demonstrate the validity of measuring Doppler shifts from line-center displacements of Ca II H & K, and we cast doubt on the significance of observed power at frequencies above $f \approx 10\,\mathrm{mHz}$ even when non-zero phase differences are observed.

2. Observations

The Vacuum Tower Telescope at the National Solar Observatory/Sacramento Peak was used to take CCD spectrograms containing:

- the extended (1 nm) blue wing of the Ca II H line. This wing contains numerous blends and "continuum" windows which permit tracing velocity and intensity fluctuations as a function of height throughout the photosphere and low chromosphere;
- the core of Ca II H, a much cleaner diagnostic for chromospheric dynamics than the Ca II infrared lines or Hα, although it is very opaque (cf. Lites *et al.*, 1993);
- He I 1083.04 nm. This line is difficult to measure in quiet regions, but it represents a reliable Doppler indicator because it is optically thin (cf. Lites, 1986).

Various sequences were obtained during October 1991, containing internetwork, network, pores, and small spots. We display a small subset of the results here.

3. Chromospheric power patterns

Figures 1 and 2 show power (actually its square root, *i.e.,* the rms amplitude of velocity fluctuations) as function of spatial position along the slit and of Fourier frequency, determined from the line-center Doppler shifts of He I 1083.0, Ca II H, the strong Al I resonance line in the H wing and a weak Fe I blend in the H wing. Larger amplitude is displayed as black. Figure 1 is from quiet Sun data while Fig. 2 is for a field with a small pore.

The quiet-Sun results in the two photospheric panels on the right in Fig. 1 show familiar changes with height in oscillation properties. The weak Fe I line has two bands of enhanced power, for p–mode oscillations (3–5 mHz) and for granulation (0–1 mHz), respectively, without network/internetwork distinction in either band. The stronger Al I line loses the granulation, but gains contribution from propagating acoustic waves with frequencies $f > 5.5\,\mathrm{mHz}$; its oscillation band stretches from 3 mHz to 7 mHz. The network is not yet distinct.

The two left-hand panels are for the overlying chromosphere. The Ca II H core shows a marked disparity between network and internetwork Doppler shift variations. Network elements primarily have long-period fluctuations in the chromosphere, best seen in the cores of the H & K lines (Lites *et al.*, 1993). The internetwork contains power primarily in the so-called 3–min band (4–8 mHz or 4–2 minute periodicity;

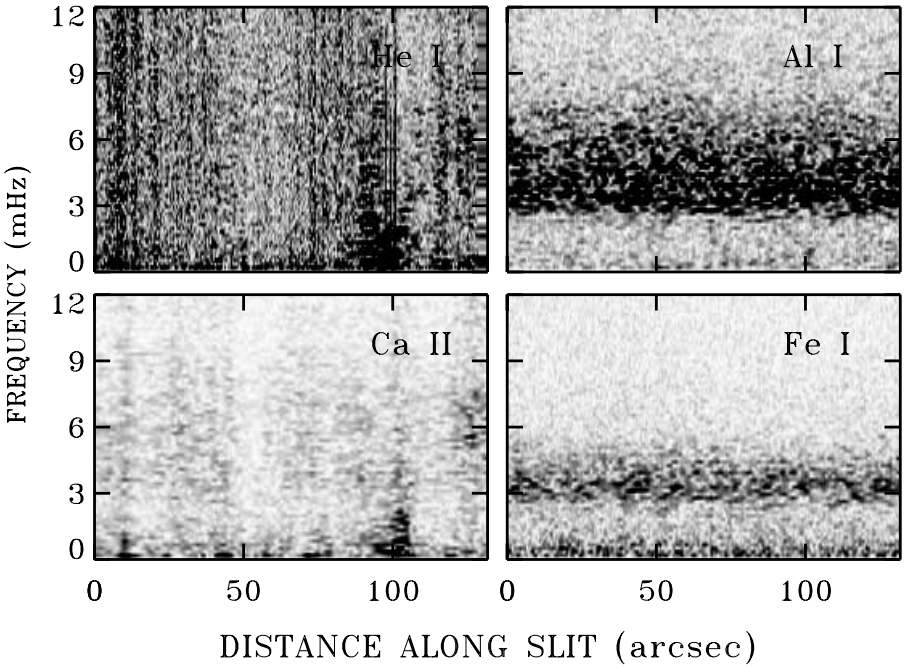

Fig. 1. Quiet-sun velocity power spectra from four lines that were registered simultaneously, respectively He I 1083.0 (upper left panel), Ca II H_3 (396.85 nm, lower left), the strong Al I 396.154 nm resonance line (upper right), and the weak Fe I 396.344 nm line (lower right). The slit crossed network around position 100, as evident in Ca II H. The striping at the far right in the He I panel is due to correction for differential refraction along the slit.

the term "3–min" denotes the whole band), but in Fig. 1 there is enhanced power in this band only on the far right. This spatial amplitude variation is our first topic of discussion.

The comparable quiet Sun display in Fig. 4 of Lites *et al.* (1993) also shows large spatial variation in the amount of 3–min power across the internetwork regime, but it is even more striking here; the internetwork regime does not show enhanced 3–min power along most of the spectrograph slit. A movie produced from simultaneous slitjaw images taken in the core of the Ca II K line shows corresponding absence of "grain" activity over the whole field except at the top, here crossed by the slit at the right. In other data sets, *e.g.,* the La Palma K_{2V} filtergram movie discussed by Brandt *et al.* (1992, and in these proceedings), similar large-scale variation in 3–min power is noticeable.

Thus, it seems that only parts of quiet Sun internetwork regions partake in the large-amplitude 3–min oscillations that produce repeated, "standard" bright Ca II K_{2V} and H_{2V} grains appearing in the repeated, well-defined development patterns (see Rutten and Uitenbroek, 1991), that are so strikingly well reproduced by the

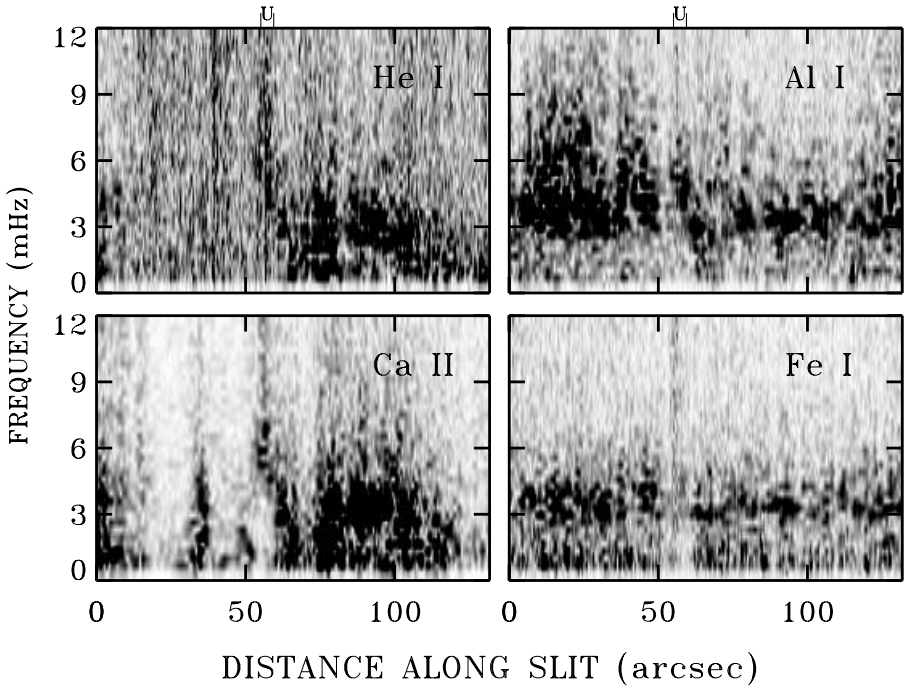

Fig. 2. Power spectra as in Fig. 1 for an area containing a small pore (marked by the symbols U at the top).

numerical radiation hydrodynamics simulations of Carlsson and Stein (1992). In fact, the wave train in the data of Lites *et al.* (1993) emulated by Carlsson and Stein is one of only a few in that data set; similarly, Fig. 2 of Kulaczewski (1992) seems to contain no regular "grain train" comparable to the patterns seen in panels 114–120 of Fig. 4 of Cram and Damé (1983). Such trains seem to be fairly rare.

The results of Sivaraman and Livingston (1982) indicate that the brighter Ca II internetwork grains are related to concentrations of internetwork field; the long-lived "persistent flasher" reported by Brandt *et al.* (1992) and discussed by Brandt *et al.* elsewhere in these proceedings is undoubtedly anchored magnetically. Deeper down, the photospheric results of Brown *et al.* (1992) show increased 3–min power near to, but just outside of, plage.

We infer that spatial variations of 3–min power may result not only from wave interference, such as between 3–min and 5–min oscillations (Rutten and Uitenbroek, 1991), between successive 3–min waves excited by a 5–min piston (Fleck and Schmitz, 1993), and between direct and once-refracted outgoing waves (Kumar, 1994; Duvall *et al.*, 1993), but also from large-scale spatial source distributions which are connected to the magnetic topology.

Fig. 2 is from a less quiet field, containing a small pore for which the symbols

U mark the spatial position of the umbra. This display is indeed more confused. The photospheric panels are less homogeneous than for the quiet Sun Fig. 1. The chromospheric panels show not much 3–min power, except for the pore, but contain much power at 5 min and longer periods at the right. The Al I panel lacks 3–min power in that area. The high–f columns at the pore location are undoubtedly due to seeing (see below).

Disentangling the complexities of these spatial power variations requires two-dimensional data sets, in large quantity to obtain sufficient statistical significance. Long sequences are needed to employ long-term migration behavior as diagnostic to identify long-lived oscillators such as the flasher described by Brandt *et al.*

4. Chromospheric velocity measurement

The upper-left panels in Figs. 1 and 2 show power spectra from He I 1083.0 Doppler shifts. They are very noisy, but nevertheless show close correspondence to the Ca II H panels. This correspondence validates the interpretation of H_3 wavelength shifts as indicative of true material motion. The Ca II H line is very opaque while the He I line is optically thin; correspondence between line-center shifts measured from these two disparate lines implies that actual Doppler shifts are indeed sampled.

We elaborate on this comparison with phase difference diagrams in Figs. 3 – 5. Fig. 3 shows phase-difference spectra between the $(R-V)/(R+V)$ ratio and line-center Doppler shift for Ca II H, where R is the H_{2R} intensity and V the H_{2V} intensity. The $(R-V)/(R+V)$ ratio is a good proxy for velocity measurement when a substantial part of the H_{2R} and H_{2V} intensity modulation is governed by the Doppler shift of the H_3 core, in particular for the "regular" internetwork H_{2V} grain evolution pattern in which the H_{2V} intensity peaks at maximum H_3 Doppler shift (Cram and Damé, 1983; Mein *et al.*, 1987). Fig. 3 shows that the $(R-V)/(R+V)$ ratio agrees closely with H_3 Doppler shift also for the network (left-hand panel) and to some extent even for an umbra (right-hand panel). In the latter, the averages depart significantly from 0°. The small error bars indicate that the two measures refer to the same atmospheric phenomenon, *i.e.,* umbral flashes in the 3–min band.

The two H-line measurements are compared to He I 1083.0 Doppler shift in Fig. 4, for the internetwork area cut by the slit to the far right in Fig. 1 where the chromospheric 3–min oscillation is relatively strong. The correspondence is good, especially in the 3–min regime where the error bars are smallest. Thus, Ca II H and He I 1083.0 measure internetwork 3–min oscillations in a similar fashion. The rms oscillation amplitudes are also comparable, respectively $1.7\,\mathrm{km\,s^{-1}}$ for H_3 and $1.1\,\mathrm{km\,s^{-1}}$ for He I 1083.0. This similarity might not be expected from standard hydrostatic formation estimates placing He I 1083.0 response at larger temperature than the Ca II H & K response (Avrett *et al.*, 1994). However, if the chromosphere is pervaded by overtaking shocks as in the simulations of Rammacher and Ulmschneider (1992) and Carlsson and Stein (1992), it is likely that sufficient opacity for detectable signal is provided by a single layer (or blob) of hydrodynamically compressed matter to both lines at the same time.

In contrast, a similar comparison between H_3 Doppler shift and He I 1083.0 Doppler shift in the left-hand panel of Fig. 5 for an umbra shows a large, frequency-

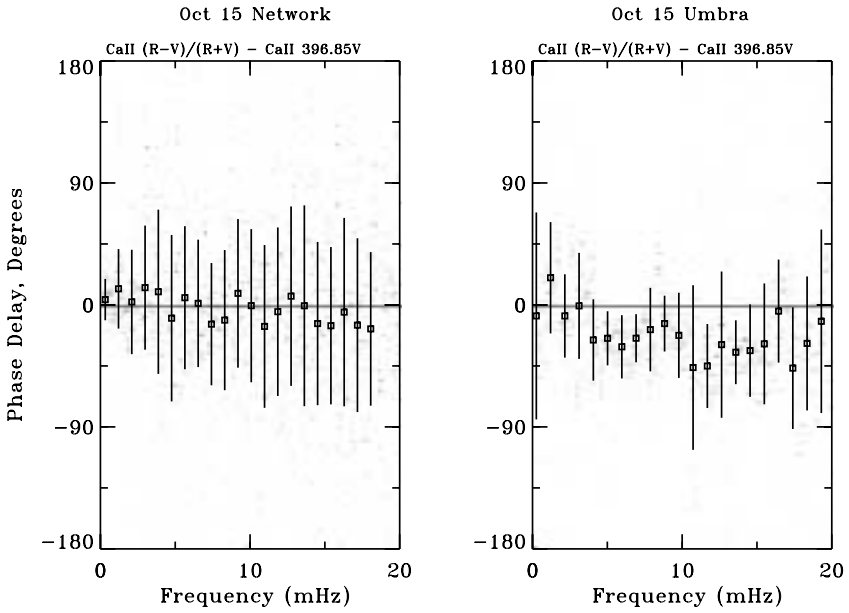

Fig. 3. Phase difference spectra between the Ca II H $(R-V)/(R+V)$ ratio and H_3 Doppler shift. Left: network. Right: umbra. The scattered points are independent determinations from different spatial positions. The bars are $1\,\sigma$ deviations from their averages (squares) per frequency bin.

dependent phase difference between the two measurements, in agreement with the results of Lites (1986) who concluded that the He I 1083.0 line is the preferred diagnostic to quantify umbral motions.

5. High-frequency signal significance

The right-hand panel of Fig. 5 shows intensity phase differences between the low and high photosphere measured from two blend-free windows in the blue wing of Ca II H. At frequencies $f > 10\,\mathrm{mHz}$, the phase differences scatter around 180°. The same is seen in the left-hand panel, but there there are also high-frequency averages near 0°. This behavior corresponds to the effect of seeing analyzed by Endler and Deubner (1983) (cf. Deubner *et al.*, 1984), "pulling phase differences to 0° or 180°". Put simply, when seeing excursions move small-scale structures on and off the slit at high speed, signals result as schematically illustrated in the left-hand panel of Fig. 6. Such jittering causes high–f power with 0° phase lag when the two measured signals are correlated at low frequency, 180° lag if the two solar signals are anti-correlated as in the illustration.

For example, image motion in $I-V$ measurements of the solar granulation adds high–f components with 0° phase lag and high coherence between I and V, because rapid granular excursions across the slit produce synchronous high–f noise spikes in both I and V, in phase because bright granules move upward. A good example of such granular jittering is shown in the Fe I $I-V$ phase and coherence spectra in

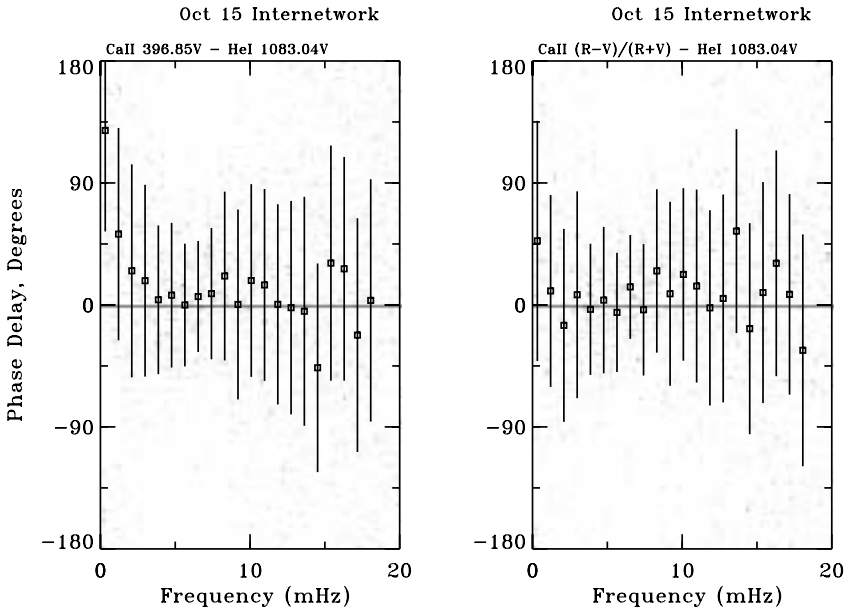

Fig. 4. Phase difference spectra for the quiet Sun internetwork at the far right in Fig. 1, respectively between H_3 Doppler shift and He I 1083.0 Doppler shift (left) and between the Ca II H $(R-V)/(R+V)$ ratio and He I 1083.0 Doppler shift (right).

the top panels of Fig. 5 of Kulaczewski (1992). The phase difference is concentrated near 0° (actually 180° in his plot because he takes velocity positive downward) both at the low frequencies where granulation dominates the signal and at the highest frequencies; the coherence between I and V is largest and equal in these two domains. Similar high–f noise from seeing jitter of granules is seen in photospheric $V-V$ and $I-I$ comparisons. Another example is given by the pore in Fig. 2. It also furnishes long-lived steep spatial signal gradients, from which seeing jitter produces spurious high–f signals with column-like appearance in such spatially-resolved power spectra. The 5–min oscillation patterns contribute less high–f noise from image motion because they have larger spatial extent.

Higher up in the atmosphere the situation changes. In the inner H-line wing, a partial contrast reversal occurs on small spatial scales (Evans and Catalano, 1972) that is attributed by Suemoto *et al.* (1987, 1990) to bright downflows above intergranular lanes. In the inner–outer wing comparison in Fig. 5 this reversal shows as negative phase lag at low frequencies. Seeing jitter of these low–f reversals across the slit produces high–f noise with 180° phase differences in the right-hand panel of Fig. 5, as it would do for the counter-correlated signals in the left-hand illustration of Fig. 6.

However, this is not the whole story. Seeing may also, while modulating low–f signals to higher frequencies, transcribe phases from low to high frequency and so produce spurious high–f signals with phase differences other than 0° or 180°. This happens for image blurring rather than image motion. The right-hand panel of Fig. 6

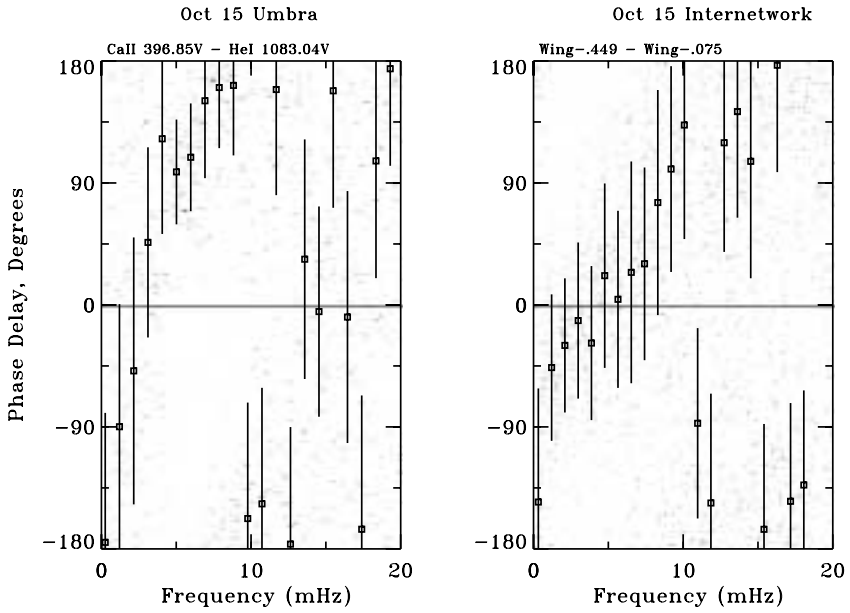

Fig. 5. Left: $V - V$ phase differences between H_3 Doppler shift and He I 1083.0 Doppler Shift for an umbra. Right: $I - I$ phase differences between the intensities at $\Delta\lambda = -0.449$ nm and -0.075 nm from H_3, for the quiet Sun internetwork pixels at the far right in Fig. 1.

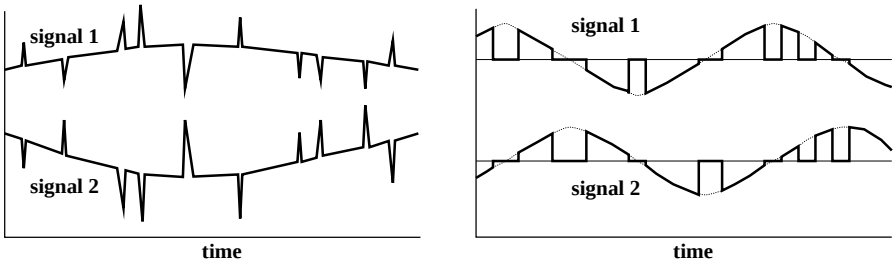

Fig. 6. Schematic illustration of seeing effects, respectively "phase pulling" by image motion and "phase aliasing" by image blurring. Left: rapid excursions of small structures with steep spatial signal gradients across the slit cause high–f components with either 0° or 180° phase difference between different co-spatial signals. Right: episodic erasures of low–f signals cause high–f components with the same phase difference as between the low–f signals.

is a schematic illustration for two monofrequent signals that are 90° out of phase, with image blurring that consists of abrupt wash-out episodes in which the image loses all structure. Such blurring constitutes multiplication by a window function, the same for both oscillations (which may be regarded as modulating the window function). Convolution of their transforms and the window transform maintains the oscillation phase difference; the high–f Fourier components that serve to reproduce the blurring episodes in the two signals therefore have the same pairwise phase lag as the low–f oscillations. Thus, blurring may alias low–f phase differences to similar

high–f phase differences. This holds also for more realistic window functions with variation in window amplitude and shape.

It is not clear whether high–f phase patterns such as those in Fig. 5 suffer more from phase pulling by image motion or from phase aliasing by image blurring, because the low–f phase differences themselves tend to $-180°$ so that both phase pulling and aliasing produce high–f differences of about that value. In other upper-photosphere and chromospheric phase comparisons, however, we have noted patterns that seem to betray phase aliasing due to blurring. We don't show them here because similar phase spectra have been published by Kulaczewski (1992). They have characteristic butterfly shapes, in which the location and spread of the low–f phase differences are mimicked at the high–f end. By and large, wide and narrow scatter correspond, the presence and absence of phase concentrations correspond, and the lag values of peak concentrations correspond as well. We therefore suspect that the high–f phase differences in these diagrams are actually set by those low–f signals which have the largest amplitude and phase stability. In particular, we wonder whether the internetwork high–f phase lags of 60–90° for Ca II 854.2 and Ca II H $I - V$ which puzzle Kulaczewski (his Fig. 6) and which have suggested "standing chromospheric waves" to Fleck and Deubner (1989) may simply be due to such aliasing of lower-frequency oscillations for frequencies $f > 10$ mHz.

Thus, high–f power should not only be distrusted when it possesses 0° or 180° phase difference, but also when high–f phase differences mimic lower–f behavior. With the advent of fast trackers and stable telescopes in Canary-quality seeing, such phase aliasing from blurring may become more noticeable than phase pulling from image motion. The two degradations differ in sensitivity to spatial structure; this difference may be an additional diagnostic.

Acknowledgements. We are much indebted to the NSO staff at Sacramento Peak, in particular the Vacuum Tower Telescope observers Steve Hegwer, Richard Mann and Eric Stratton. Jo Bruls and Gianna Cauzzi helped to transfer tapes to Exabytes. RJR gratefully acknowledges not only NATO's funding of the present workshop, but also travel support from NATO in the form of CRG grant 900229.

References

Avrett, E. H., Fontenla, J. M., and Loeser, R.: 1994, in D. M. Rabin, J. T. Jefferies, and C. Lindsey (Eds.), *Infrared Solar Physics*, Proc. IAU Symp. 154, Kluwer, Dordrecht, p. 35

Ayres, T. R.: 1991, in P. Ulmschneider, E. Priest, and B. Rosner (Eds.), *Mechanisms of Chromospheric and Coronal Heating*, Heidelberg Conference, Springer Verlag, Berlin, p. 228

Brandt, P. N., Rutten, R. J., Shine, R. A., and Trujillo Bueno, J.: 1992, in M. S. Giampapa and J. A. Bookbinder (Eds.), *Cool Stars, Stellar Systems, and the Sun*, Proc. Seventh Cambridge Workshop, ASP Conf. Ser., Vol. 26, p. 161

Brown, T. M., Bogdan, T. J., Lites, B. W., and Thomas, J. H.: 1992, *Astrophys. J.* **394**, L65

Carlsson, M. and Stein, R. F.: 1992, *Astrophys. J.* **397**, L59

Cram, L. E. and Damé, L.: 1983, *Astrophys. J.* **272**, 355

Deubner, F.-L., Endler, F., and Staiger, J.: 1984, *Mem. Soc. Astron. Italia* **55°**, 135

Duvall, T. L., Jefferies, S. M., Harvey, J. W., and Pomerantz, M. A.: 1993, *Nature* **362**, 430

Endler, F. and Deubner, F.-L.: 1983, *Astron. Astrophys.* **121**, 291

Evans, J. W. and Catalano, C. P.: 1972, *Solar Phys.* **27**, 299

Fleck, B. and Deubner, F.-L.: 1989, *Astron. Astrophys.* **224**, 245

Fleck, B. and Schmitz, F.: 1993, *Astron. Astrophys.* **273**, 671

Kalkofen, W., Rossi, P., Bodo, G., and Massaglia, S.: 1994, *Astron. Astrophys.* **284**, 976

Kulaczewski, J.: 1992, *Astron. Astrophys.* **261**, 602
Kumar, P.: 1994, *Astrophys. J.* **428**, 827
Lites, B. W.: 1986, *Astrophys. J.* **301**, 1005
Lites, B. W.: 1992, in J. H. Thomas and N. O. Weiss (Eds.), *Sunspots: Theory and Observations*, NATO ASI Series C 375, Kluwer, Dordrecht, p. 261
Lites, B. W., Rutten, R. J., and Kalkofen, W.: 1993, *ApJ* **414**, 345
Mein, P., Mein, N., Malherbe, J. M., and Damé, L.: 1987, *Astron. Astrophys.* **177**, 283
Rammacher, W. and Ulmschneider, P.: 1992, *Astron. Astrophys.* **253**, 586
Rutten, R. J. and Uitenbroek, H.: 1991, *Solar Phys.* **134**, 15
Schrijver, C. J.: 1992, *Astron. Astrophys.* **258**, 507
Sivaraman, K. R. and Livingston, W. C.: 1982, *Solar Phys.* **80**, 227
Suemoto, Z., Hiei, E., and Nakagomi, Y.: 1987, *Solar Phys.* **112**, 59
Suemoto, Z., Hiei, E., and Nakagomi, Y.: 1990, *Solar Phys.* **127**, 11